1746
doi:10.1017/S1431927622006924
Microsc. Microanal. 28 (Suppl 1), 2022

Layer Stacking Determination in Topological Semimetal $MoTe_2$ via STEM Imaging, Liquid He TEM, and Quantitative Electron Diffraction

James L Hart[1,2], Lopa Bhatt[3], Myung-Geun Han[4], David Hynek[2], John A Schneeloch[5], Yu Tao[5], Despina Louca[5], Yimei Zhu[4], Lena F Kourkoutis[3,6], Judy J Cha[1,2*]

[1.] Department of Materials Science and Engineering, Cornell University, Ithaca, NY, United States.
[2.] Energy Sciences Institute, Yale University, New Haven, CT, United States.
[3.] School of Applied and Engineering Physics, Cornell University, Ithaca, NY, United States.
[4.] Condensed Matter Physics and Materials Science Department, Brookhaven National Laboratory, Upton, NY, United States.
[5.] Department of Physics, University of Virginia, Charlottesville, VA, United States.
[6.] Kavli Institute at Cornell for Nanoscale Science, Cornell University, Ithaca, NY, United States.
*Corresponding author: jc476@cornell.edu

The precise nature of layer stacking arrangements in van der Waals solids can have profound effects on material properties. Here, we study octahedrally coordinated $MoTe_2$. In bulk, two primary layer stacking arrangements exist (Fig. 1a): the high temperature 1T' phase (an inversion-symmetric higher order topological insulator) and the low temperature T_d phase (a ferroelectric Weyl semimetal), with a bulk transition temperature of $T_c \sim 250$ K between the two phases. In thin exfoliated flakes of $MoTe_2$, the preferred layer stacking (and its temperature dependence) is hotly debated [1-3]. $MoTe_2$ flakes show exciting quantum phenomena such as exotic superconductivity and third-order non-linear Hall effect [4,5], but our understanding of this behavior is incomplete, given the uncertain sample symmetry and topology. Here, using (S)TEM imaging and diffraction, in conjunction with liquid He cooling and quantitative multi-slice modeling, we show that the layer stacking in thin exfoliated flakes of $MoTe_2$ is highly disordered, thus following neither of the bulk stacking arrangements, irrespective of temperature. The methods described herein are applicable to a number of 2D quantum materials.

First, we determine the room temperature stacking in thin exfoliated flakes of $MoTe_2$ with STEM-ADF imaging of FIB prepared cross-sectional samples. For reference images of the 1T' and T_d stacking arrangements, we study lift-outs from a bulk crystal of $MoTe_2$ (1T' phase at room temperature) and WTe_2 (T_d phase at room temperature). The position of each Te column is determined with a 2D Gaussian fit, then the inter-layer Te-Te bonds are calculated, and the in-plane bond component is represented with overlaid arrows. As shown in Fig. 1a, the bulk $MoTe_2$ crystal shows the expected 1T' stacking (↑↑↑↑), and the bulk WTe_2 crystal shows the expected T_d stacking (↑↓↑↓). In sharp contrast, for a ~10 nm thick flake of $MoTe_2$ – exfoliated from the same bulk $MoTe_2$ crystal imaged in Fig. 1a – we observe mixed 1T' and T_d stacking, along with regions of highly disordered stacking (Fig. 1b). The layer stacking varies at solitons, as marked with the white arrow (Fig. 1c). This data provides the first direct characterization of layer stacking in exfoliated $MoTe_2$.

Resistivity data of exfoliated $MoTe_2$ flakes suggest layer sliding events down to < 50 K, thus, to study the temperature-dependence of layer stacking, we use liquid He TEM. We find that layer sliding is quenched in FIB prepared samples, and instead, it is necessary to study flakes in plan-view. With this geometry, the disordered stacking along [001] prevents direct STEM image interpretation. Electron diffraction faces similar challenges, since there is no change in the (H, K, 0) diffraction plane symmetry as a function of layer stacking (because the in-plane structure is constant). However, the different

stacking arrangements alter the (*H*, *K*, 0) structure factors, allowing the layer stacking to be inferred via the spot intensities. As such, we developed a quantitative electron diffraction approach, where experimental diffraction data is fit to multi-slice simulations using four fitting parameters: flake thickness (*z*), mis-orientation about the [001] axis (α and β), and flake bending. To demonstrate the validity of our approach, we first studied exfoliated WTe_2, which possesses ordered T_d stacking. Using the T_d stacking model, we plot the fitted χ^2 for WTe_2 as a function of simulation thickness, and observe a minimum at ~ 22 nm, in excellent agreement with the EELS ZLP flake thickness of 25 ± 5 nm (Fig. 2b). For the best T_d fit (z = 22 nm), we observe excellent agreement between the experimental and simulated diffraction data across the entire fit range of $|H| < 6$ and $|K| < 4$ (Fig. 2c, panel 1).

Next, we apply our method to a ~35 nm thick $MoTe_2$ flake (Fig. 2c, panels 2-4). At room temperature, the data is best fit with a random stacking model (labeled Rnd), where the shift direction from one layer to the next is randomly generated. This fit is consistent with our cross-sectional STEM data (Fig. 1b). Upon cooling to ~17 K, subtle changes in the diffraction pattern intensity are observed, suggestive of layer stacking changes. At this temperature, the best fit is achieved with a stacking arrangement which lacks long-range order, but possesses T_d-like local order (labeled T_d-Rnd, see schematic in Fig. 2e). Our fitting results are supported by qualitative Laue zone analysis (Fig. 2d). For the WTe_2 flake with ordered T_d stacking, we see a strong first order Laue zone, reflective of a 1.4 nm *c*-lattice parameter. For the $MoTe_2$ at room temperature, no Laue zone is observed, indicative of disordered stacking which lacks a well-defined *c*-lattice parameter. At 17 K, the $MoTe_2$ flake develops a weak Laue zone, consistent with weakly ordered T_d stacking.

We demonstrated that layer stacking in thin exfoliated flakes of $MoTe_2$ differs strongly from stacking in the bulk. This data is relevant to our understanding of exotic superconductivity and other quantum properties measured in $MoTe_2$ devices [4,5]. Our quantitative electron diffraction approach, which fully accounts for dynamical scattering in thick, high *Z* materials, offers a novel way to study layer sliding transitions in van der Waals materials with *in situ* TEM.

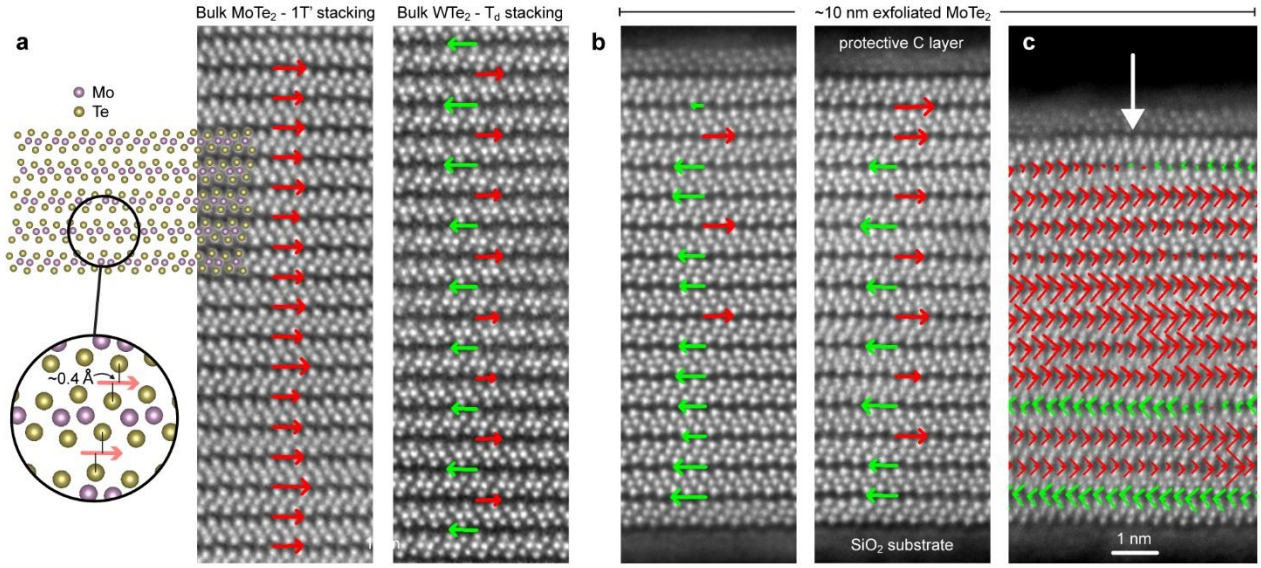

Figure 1. a) STEM-ADF images of bulk $MoTe_2$ and WTe_2, which at room temperature adopt the 1T' and T_d stacking arrangements, respectively. The overlaid arrows show the direction and magnitude of

https://doi.org/10.1017/S1431927622006924 Published online by Cambridge University Press

the measured inter-layer shift, as shown in the atomic cartoon. **b,c)** Layer shifts measured in exfoliated $MoTe_2$. Relative to bulk, the stacking is highly disordered. In **c**, the arrows show the measured shift for each individual Te-Te bond, highlighting a stacking soliton (white arrow). For **a** and **b**, the shift is averaged across all Te-Te bonds in the field-of-view. The scale bar in **c** applies to **a** and **b** as well.

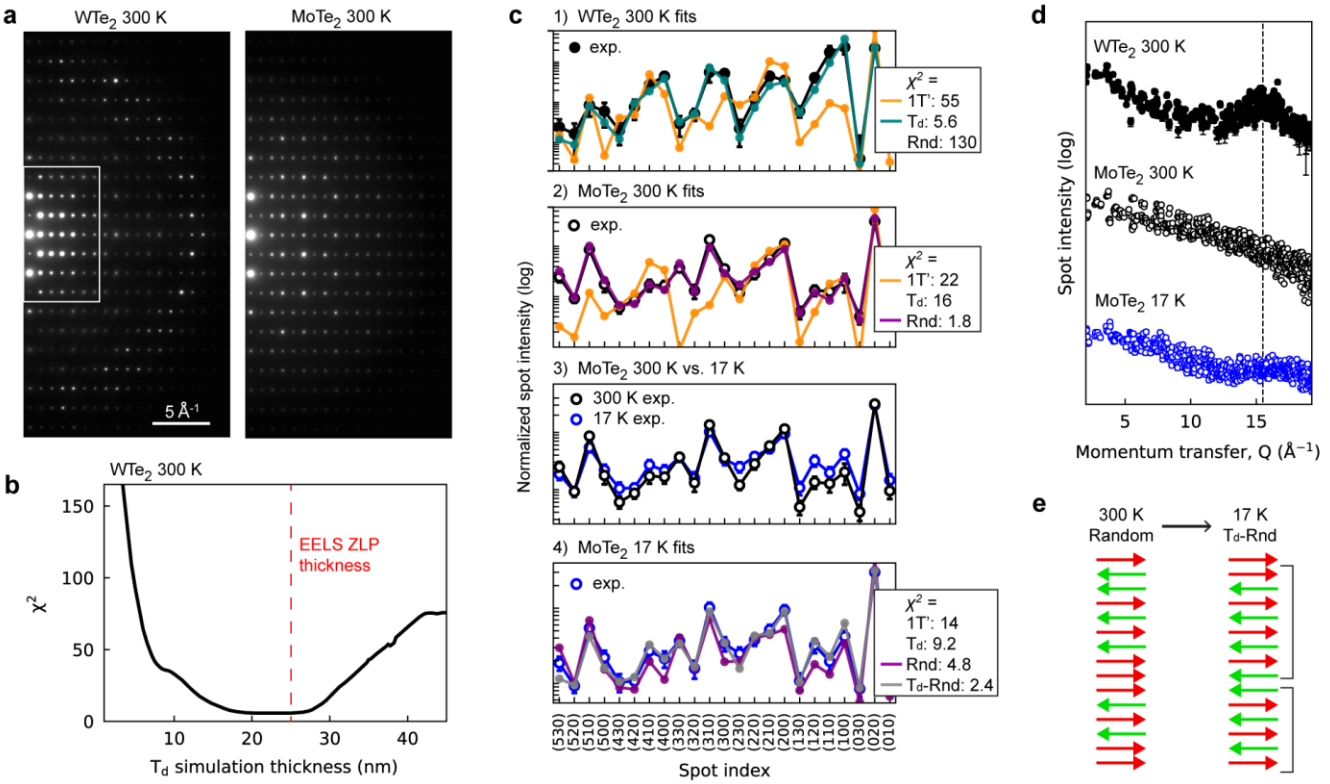

Figure 2. a) Plan-view diffraction of exfoliated WTe_2 and $MoTe_2$ flakes at ~300 K. The white box marks the (*H*, *K*, 0) spots included in our fitting procedure. **b)** Goodness of fit for the WTe_2 diffraction data as a function of the T_d simulation thickness. **c)** Results from our quantitative diffraction fitting. Panel **c1** is a demonstration on WTe_2, with the same data shown in **b**. Panels **c2-c4** correspond to a $MoTe_2$ liquid He experiment. Note that during the fitting procedure, all measured spots are treated independently, but for plotting, we average together (*H*, *K*, 0) spots of the same family. **d)** Spot intensities as a function of *Q*, showing the presence or absence of the first order Laue zone, which qualitatively reflects the degree of out-of-plane ordering. **e)** Example stacking arrangements of the Rnd and T_d-Rnd models. For the T_d-Rnd model, the brackets show local T_d domains. For fitting with these models, dozens of stacking arrangements were generated, their simulated diffraction intensities averaged together, and then compared to the experimental data.

References:

[1] R He *et al*, Phys. Rev. B. **97** (2018), 041410(R). doi.org/10.1103/PhysRevB.97.041410
[2] Y Cheon *et al*, ACS Nano. **15** (2021), p. 2962-2970. doi.org/10.1021/acsnano.0c09162
[3] B Su *et al*, Advanced Science. (2021), 2101532. doi.org/10.1002/advs.202101532
[4] W Wang *et al*, Science. **368** (2020), 534-537. doi.org/10.1126/science.aaw9270
[5] S Lai *et al*, Nat. Nano. **16** (2021), p. 869-873. doi.org/10.1038/s41565-021-00917-0

https://doi.org/10.1017/S1431927622006924 Published online by Cambridge University Press